

AD-A091 613

HONEYWELL INC. GOLDEN VALLEY MINN CERAMICS CENTER
MANUFACTURING METHODS AND TECHNOLOGY FOR OPTICAL FABRICATION.(U)
MAR 80 W B HARRISON, G HENDRICKSON, F JOHNSON DAAB07-77-C-0615

F/G 17/8

UNCLASSIFIED

47356

NL

AL
ADP 17

END

DATE

FILED

12 80

DTIC

AD A091613

80 10 27 131

DISCLAIMER STATEMENT

"The findings in this report are not be construed as official Department of the Army position unless so designated by other authorized documents."

DISPOSITION INSTRUCTIONS

"Destroy this report when it is no longer needed. Do not return it to the originator."

ACKNOWLEDGEMENT

"This project has been accomplished as part of the U.S. Army Manufacturing and technology Program, which has as its objective the timely establishment of manufacturing processes, techniques or equipment to ensure the efficient production of current or future defense programs."

UNCLASSIFIED

SECURITY CLASSIFICATION OF THIS PAGE (When Data Entered)

REPORT DOCUMENTATION PAGE		READ INSTRUCTIONS BEFORE COMPLETING FORM
1. REPORT NUMBER Interim Technical Report No. 1	2. GOVT ACCESSION NO. AD-A092	3. RECIPIENT'S CATALOG NUMBER 613
4. TITLE (and Subtitle) Manufacturing Methods and Technology for Optical Fabrication	5. TYPE OF REPORT & PERIOD COVERED Interim 28 Sept - 30 August 1978	
7. AUTHOR(s) William B. Harrison	6. PERFORMING ORG. REPORT NUMBER 47356	
9. PERFORMING ORGANIZATION NAME AND ADDRESS Defense Electronics Division Ceramics Center Golden Valley, Minnesota 55422	8. CONTRACT OR GRANT NUMBER(s) DAAB07-77-C-0615	
11. CONTROLLING OFFICE NAME AND ADDRESS Technical Support Activity - USAERADCOM Fort Monmouth, New Jersey	10. PROGRAM ELEMENT, PROJECT, TASK AREA & WORK UNIT NUMBERS Project No. 2779845	
14. MONITORING AGENCY NAME & ADDRESS (if different from Controlling Office)	12. REPORT DATE	
	13. NUMBER OF PAGES	
	15. SECURITY CLASS. (of this report) UNCLASSIFIED	
	15a. DECLASSIFICATION/DOWNGRADING SCHEDULE	
16. DISTRIBUTION STATEMENT (of this Report) Approval for public release; distribution unlimited.		
17. DISTRIBUTION STATEMENT (of the abstract entered in Block 20, if different from Report)		
18. SUPPLEMENTARY NOTES		
19. KEY WORDS (Continue on reverse side if necessary and identify by block number) IR Optics, Optical Fabrication, Single Point Diamond Turning, Form-to-Shape Optics, FLIR Systems, Optical Testing		
20. ABSTRACT (Continue on reverse side if necessary and identify by block number)		

DD FORM 1473

1 JAN 73

EDITION OF 1 NOV 65 IS OBSOLETE

UNCLASSIFIED

SECURITY CLASSIFICATION OF THIS PAGE (When Data Entered)

9 INTERIM TECHNICAL REPORT, NO. 1
28 Sep 77-30 Aug 78

PROCESS ANALYSIS

15 CONTRACT NO. DAAB07-77-C-0615

6 Manufacturing Methods and Technology
for Optical Fabrication,

Accession For	
NTIS GRA&I	<input checked="" type="checkbox"/>
DDC TAB	<input type="checkbox"/>
Unannounced	<input type="checkbox"/>
Justification	
By	
Distribution/	
Availability Codes	
Dist.	Avail and/or special
A	

PERIOD COVERED: 28 September 1977--30 August 1978

10 PREPARED BY:

William B.
W./Harrison
G./Hendrickson
F./Johnson
I./Abel
J./Starling

12 62

11 Mar 80

14 47356

OBJECT:

The overall objective of this contract is to establish cost-effective lens fabrication techniques for germanium operating in the 8-12 micrometer wavelength. The specific objective of the first task discussed in this report was to establish the materials and processes necessary for the production of more cost-effective germanium lenses typical of those required for advanced forward looking infrared systems.

DISTRIBUTION STATEMENT

UNCLASSIFIED: "Approval for public release; distribution unlimited."

409443

PURPOSE

This Manufacturing Methods and Technology (MM&T) contract was undertaken to establish improved methods for producing the spherical and aspheric germanium lenses required for Forward Looking Infrared (FLIR) systems. Current systems primarily use germanium elements with spherical surfaces that can be made by conventional lens fabrication techniques; however, such elements are very expensive. Germanium requires wasteful grinding and laborious finishing and inspection operations. In addition, conventional systems require more elements--a total of about nine, versus the six or seven used in an aspherical system. Efficient production techniques for aspherical optical surfaces, however, have not been available, and their high cost may limit their advantages.

By studying form-to-shape and precision machining optical fabrication techniques that minimize the use of germanium and reduce conventional optical finishing, this program will determine cost-effective ways of producing both spherical and aspheric surfaces. Seven lenses and one mirror will be fabricated, assembled, and tested to meet the drawing and specification requirements established for this contract.

➤ The major tasks of this program consist of (1) delivery of samples produced by four different processes representing conventional, precision machining and form-to-shape approaches; (2) delivery of 36 lenses made by the most cost-effective approach; identified in Task 1; (3) delivery of four aspheric aluminum mirrors produced by single point diamond turning; and (4) delivery of eight sets of optical elements that have been assembled and tested. ↵

TABLE OF CONTENTS

SECTION	TITLE	PAGE
1	INTRODUCTION	1-1
2	ENGINEERING APPROACH	2-1
2.1	PROBLEM DEFINITION	2-1
2.2	EXPERIMENTAL APPROACH.	2-1
2.3	FABRICATION PROCESSES.	2-2
	2.3.1 Raw Material Source.	2-4
	2.3.2 Raw Material Evaluation.	2-4
	2.3.3 Infrared Transmission.	2-4
	2.3.4 Electrical Resistivity	2-7
	2.3.5 Mechanical Strength.	2-7
	2.3.6 Microstructure	2-8
	2.3.7 Optical Absorption Coefficient	2-8
	2.3.8 Preshape Fabrication	2-8
	2.3.9 Conventional Preshaping.	2-9
	2.3.10 Casting.	2-9
	2.3.11 Hot Deformation.	2-9
	2.3.12 Casting and Hot Deformation.	2-9
	2.3.13 Optical Finishing.	2-11
	2.3.14 Conventional Polishing	2-11
	2.3.15 Single Point Diamond Turning	2-11
	2.3.16 Testing and Evaluation	2-13
	2.3.17 Flatness	2-13
	2.3.18 Optical Transfer Function (OTF).	2-13
	2.3.19 Cost Analysis.	2-15
3	RESULTS AND DISCUSSION	3-1
3.1	CONVENTIONAL LENS GENERATING PROCESSES	3-1
3.2	HOT DEFORMATION AND CASTING PROCESSES.	3-4
	3.2.1 Comparison Between Deformation of Alkali Halides and Germanium.	3-4
	3.2.2 Hot Deformation of Germanium Discs	3-5
	3.2.3 Casting and Hot Deforming of Germanium Lens Blanks	3-8
	3.2.4 Polishing and Single Point Diamond Turning of Germanium.	3-8
	3.2.5 Evaluation of Optically Polished Germanium	3-11
3.3	COST ANALYSIS.	3-15
4	CONCLUSIONS.	4-1
5	RECOMMENDATIONS.	5-1

TABLE OF CONTENTS (Continued)

APPENDIX	TITLE	PAGE
A	REFERENCES	A-1
B	GLOSSARY OF TERMS.	B-1
C	DETAILED COST FIGURES FOR MANUFACTURING METHODS AND TECHNOLOGY FOR OPTICAL FABRICATION	C-1
D	DISTRIBUTION LIST.	D-1

LIST OF ILLUSTRATIONS

FIGURE	TITLE	PAGE
2-1	Curve Generated Germanium Hot Forging Blanks	2-6
2-2	Hot Deforming Apparatus.	2-10
2-3	Single Point Diamond Turning (SPDT) of Four-Surface Mirror	2-12
2-4	OTF Test Equipment Setup	2-14
3-1	Present Germanium Lens Fabrication Flow Diagram.	3-2
3-2	Lens Forming From Germanium Blank.	3-3
3-3	Conventional Methods of Generating Lenses.	3-3
3-4	Deformation Mechanism Map for Germanium.	3-6
3-5	Hot Deformation of Lens.	3-9
3-6	Germanium Lens Blanks (a) Casting, (b) Hot Deformed. . . .	3-10
3-7	Photomicrographs of Finished Germanium (x 200 Magnifica- tion).	3-12
3-8	Plots of Infrared Optical Transmission of Germanium. . . .	3-13

LIST OF TABLES

TABLE	TITLE	PAGE
2-1	LENS SPECIFICATION.	2-3
2-2	GERMANIUM MATERIAL.	2-5
3-1	PROCESS DATA ON OPTICAL EVALUATION PARTS.	3-7
3-2	OTF DATA.	3-16
3-3	MMAT COST ANALYSIS SUMMARY.	3-17

APPENDIX	TITLE	PAGE
C	FACTORY COST BREAKDOWN FOR PROCESS A - CASTING.	C-2
	FACTORY COST BREAKDOWN FOR PROCESS B - DEFORMING.	C-3
	FACTORY COST BREAKDOWN FOR PROCESS C - PRESHAPED.	C-4
	FACTORY COST BREAKDOWN FOR PROCESS D - CONVENTIONAL	C-5

SECTION 1

INTRODUCTION

This MM&T program focused on the needs for low-cost germanium optical fabrication approaches suitable for the afocal telescope and the IR-imager used in FLIR systems where the number of lenses in the system has been minimized by the use of aspheric surfaces to produce a lighter weight, more compact system.

A forward Looking Infrared (FLIR) System is a thermal imaging approach of scanning for infrared emission, typically in the 3 to 5 μm or 8 to 12 μm region. This system has demonstrated its performance in a variety of day and night sensors for military surveillance and tracking systems. The target being scanned emits a radiation signature that is amplified and then displayed on a real-time basis. Dual afocal telescope modules with a wide angle and narrow angle field of view for target acquisition and identification, respectively, concentrate the emission on the IR imaging optics, which focus the signal on a cryogenically cooled detector array. A mirror scanning mechanism is also required to produce the complete display.

The high cost associated with the optical components in present FLIR systems operated in the 8 to 12 μm wavelength has and will be one of the primary limitations as to how extensively these systems will be deployed by DoD. Dozens of different optical designs have evolved from the various developers of these systems. There is now a concentrated effort to modularize and reduce the variety of optical assemblies down to a few standard modules. Such an effort by the Army's Night Vision Laboratory on the IR imager has already been accomplished. However, each FLIR system still requires a different interchangeable pair of afocal telescopes for narrow angle and wide fields of view. Each of these telescopes contains about four optical lenses made primarily from germanium.

In addition to modularization, other workers have made significant progress in reducing the high cost associated with these optical systems. Aspheric surfaces have been utilized in a RPV (Remotely Piloted Vehicle) FLIR System to eliminate several spherical lenses.² Both substantial material cost and weight savings have been realized with this approach. The higher cost of producing aspheric surfaces, however, needs the further attention of this current MM&T effort. (See the first quarterly¹ report for a more detailed description of this program.)

In this first Interim Report the current processes used to manufacture germanium lenses are examined and several approaches are evaluated for producing more cost-effective spheric and aspheric lenses. These include hot deformation, casting, pre-shaping and single point diamond turning.

SECTION 2

ENGINEERING APPROACH

The overall engineering approach that is being pursued in this program was described in the first quarterly report.¹ The contracting officer agreed that subsequent reports will be written only at the completion of each of the four major tasks on the program: (1) Process Analysis (2) Lens Fabrication (3) Mirror Fabrication and (4) Lens/Mirror Assembly and Testing. This first interim report describes the work performed on Task 1.0 --Process Analysis, and covers the period from 28 September 1977 through 30 August 1978. Several contract modifications were made during the period of August 1978 to January 1979 and the contract effort was discontinued during this period.

2.1 PROBLEM DEFINITION

The optical manufacturing processes used to fabricate both spheric and aspheric germanium infrared lenses have been so expensive that widespread deployment of these systems has not been feasible. Several systems, such as the large and small common modular IR-imager, have been established which use spheric lens elements; however, no production systems have been produced with aspheric lenses. The use of aspherics would in many instances reduce the number of lenses required in a system and thereby reduce the amount of material and weight in the system. The optical fabrication, control and optical measurements required for producing aspheric surfaces are very labor intensive processes. Automatic controlled fabrication processes need to be established for generating the final aspheric optical figure required. More effective use of the germanium material also needs to be made.

2.2 EXPERIMENTAL APPROACH

The optical fabrication processes to be established in this program are for six aspheric lenses, one spheric germanium lens, and one aluminum

aspheric mirror. General specifications for these items are given in Table 2-1. Two of the aspheric lenses, AB108-1 and 2, will be produced for demonstration purposes only; however, the mirror and other five lenses will be suitable for a complete FLIR system.

The AB114-1 and 2 lenses will be used for a two element IR-imager. A wide angle field-of-view afocal assembly will use one AB116-1 mirror and one AB116-2 lens and the AB115-1 and 2 lenses will be used for a narrow angle field-of-view afocal assembly. Thus, a smaller, lighter FLIR system will be demonstrated which has only five lenses as opposed to the seven spheric lenses used in current FLIR systems.

In this first task, methods were studied which would conserve germanium and maximize the cost effectiveness of the optical fabrication process. An economical source and shape of germanium material was established by examining four methods of forming the germanium blank used for final optical finishing. Conventional optical finishing and numerically controlled single point diamond turning were examined and evaluated for each of the four methods used to form the initial optical blanks. An extensive cost analysis was then made and used to select the most appropriate approach to be pursued in Task 2 for each lens.

2.3 FABRICATION PROCESSES

A review of the current processes which are used to fabricate and evaluate spheric and aspheric germanium lenses was given in the first quarterly report¹. This section will discuss the four specific methods that were used in Task I to determine the most economical approach to form the starting germanium optical blanks subsequently used for conventional optical polishing or single point diamond turning finishing operations required for the spheric or aspheric optical surfaces.

TABLE 2-1. LENS SPECIFICATION

Lens	Diameter (inches)	Center Thickness (inches)	Minimum Clear Aperture (inches)	Spherical Radius (inches)	Surface Key/No.	Maximum Test Plate Fit Fringes at 6328Å	Maximum Astig. Fringes at 6328Å	Best Fit Spherical Radius for Aspheric Surface Inches	Spherical Maximum Departure Fringes at 6328Å
AB114-1	2.800 +0.000 -0.002	0.200 ± 0.002	2.400	Aspheric 3.0197 ± 0.0002	5/R ₁ 6/R ₂	4	2	2.6499	24
AB114-2	1.800 +0.000 -0.002	0.192 ± 0.002	1.600	1.310 ± 0.008 1.411 ± 0.008	7/R ₁ 8/R ₂	4 4	2 2		
AB115-1	2.000 +0.000 -0.002	0.100 ± 0.002	1.800	Aspheric 1.008 ± 0.008	9/R ₁ 10/R ₂	4	2	1.2203	53
AB115-2	2.000 +0.000 -0.002	0.190 ± 0.002	1.800	-1.6919 ± 0.0000 Aspheric	11/R ₁ 12/R ₂	4	2	-1.6727	5.6
AB116-1	6.200 +0.000 -0.002	0.80 min	6.000	Aspheric Mirror	13/R ₁			-16.1031	30
AB116-2	2.50 ± 0.02	0.250 ± 0.002	2.30	-6.1883 ± 0.0008 Aspheric	15/R ₁ 16/R ₂	4	2	-3.6434	24
AB108-1	3.260 +0.000 -0.002	0.300 ± 0.002	3.00	Aspheric -41.250 ± 0.08	1/R ₁ 2/R ₂	4	2	41.2901	3.6
AB108-2	1.000 ± 0.001	0.110 ± 0.005	0.90	2.153 ± 0.002 Aspheric	3/R ₁ 4/R ₂	5	2	2.4035	89

Chamfer 45° ± 5°
 Face Width 0.020 ± 0.010
 Centering ± 0.0005 FIR

Surface Finish 80/50
 AR Coating MLAR 306

2.3.1 Raw Material Source

Germanium was ordered from Eagle-Picher Industries² and Exotic Material³ in several different forms. Table 2-2 gives a list of the materials obtained from each of these vendors. The 1.5" diameter Eagle-Picher disc was diamond sawed into two discs about 0.23 inch thick and then ground to the convex/concave shape shown in Figure 2-1a. A Model No. 5 Elgin Curve generator was used with a one-inch radius (r) diamond cup wheel rotated at about 700 rpm. The angle of tilt θ , as calculated from Equation (1), was adjusted to yield a radius (R) on the germanium blank of about 5.6 inches.

$$\sin \theta = \frac{r}{R} \quad (1)$$

The one-inch diameter convex/concave shaped blanks were obtained from Exotic Materials. Both the standard Bridgeman processed material and cast material were ground to the shape shown in Figure 2-1b. All of the cast germanium blanks were cut from larger directionally solidified cast material as opposed to multi-crystalline larger Bridgeman grown ingots.

2.3.2 Raw Material Evaluation

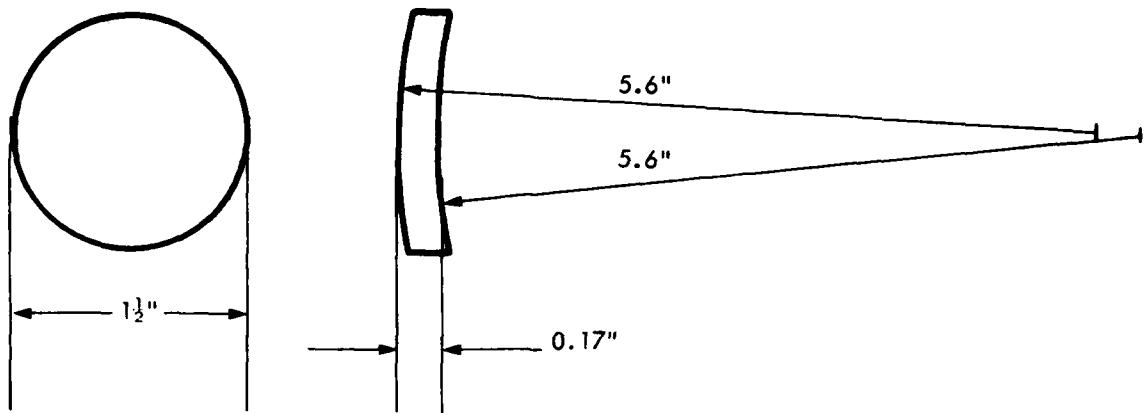
A sample of each type of IR optical grade germanium was evaluated to establish its conformance to SM-C-804148¹. Infrared transmission, electrical resistivity, optical absorption coefficient, physical strength, and microstructure were assessed by the techniques described below.

2.3.3 Infrared Transmission

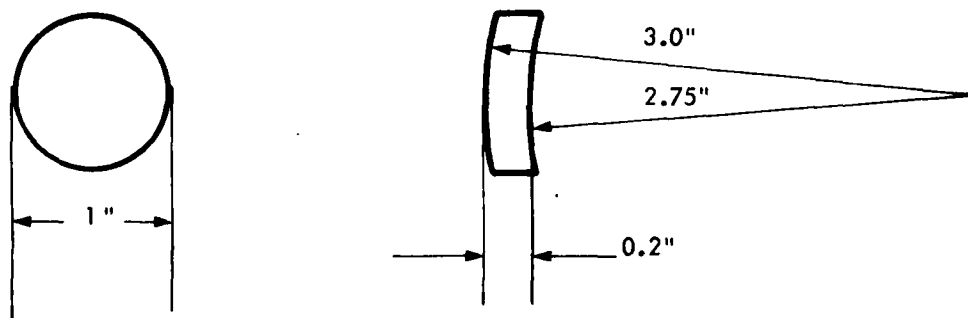
A Digilab FTS-14 infrared spectrometer, which is a Fourier transform type of instrument, was used for the analysis of each type of germanium acquired for this program. The FTS-14 is an interferometric spectrometer capable of 0.5 cm^{-1} resolution over a useful range of 10,000 cm^{-1} (1 μm) to 50 cm^{-1} (200 μm). It has greater optical throughput than a standard dispersive

Table 2-2. GERMANIUM MATERIAL

FORM OF GERMANIUM	SOURCE	QUANTITY
99.999% Ge 100 mesh, 1st reduction powder	Eagle-Picher	1000 gm
1.5 inch diameter by 0.5 inch thick disc- IR grade Bridgeman	Eagle-Picher	3
1.0 inch diameter convex/concave ground blanks - - IR grade Bridgeman	Exotic Materials	6
1.0 inch diameter convex/concave cast blanks - - IR grade	Exotic Materials	6
1.0 inch diameter by 0.2 inch thick disc- IR grade Bridgeman	Exotic Materials	6
1.0 inch diameter by 0.2 inch thick disc- IR grade - - cast blanks	Exotic Materials	6
Bridgeman Ingot	Exotic Materials	1000 gm



a. ONE AND ONE HALF INCH EAGLE - PICHER



b. ONE INCH EXOTIC MATERIALS, INC.

Figure 2-1. Curve Generated Germanium Hot Forging Blanks

spectrometer, thereby allowing a dramatic improvement in the signal-to-noise ratio obtained. Data obtained is stored in a dedicated Data General Nova 1200 computer. All of the samples evaluated were 0.1 to 0.5 thick. Since these samples were not antireflectively coated, the observed transmission (T_0) had to be corrected for the index of refraction (n) for germanium which was assumed to be 4.003 by Equation (2):

$$\% \text{ transmission} = \frac{T_0 (1+n^2)}{2n} \quad (2)$$

2.3.4 Electrical Resistivity

The electrical resistivity of three polished bars (with a width (w) and thickness (t) of 0.12 x 0.08 inch) from each type of germanium was determined by the common four-point probe method. A voltage (V_1) of 1.5 volts was applied to the end electrodes which were a length L_1 apart and the current (I) was measured. The voltage drop (V_2) between the inter two electrodes at a length (L_2) apart was then measured. Equation (3) was used to calculate the specific resistivity:

$$\rho = \frac{wtV_2}{L_2 I} \quad (3)$$

2.3.5 Mechanical Strength

The samples used for the electrical resistivity measurements were optically polished to remove all visible signs of surface damage and then the bonding strength was determined with a 3-point loading. The load (P) was applied at a rate of 0.002 in/in/min to the center of a bar supported on a 0.64 inch span (L) until the sample fractured. The modulus of rupture (σ) was then calculated by Equation (4)

$$\sigma = \frac{3PL}{2bh^2} \quad (4)$$

where b is the width and h the thickness of the bar.

2.3.6 Microstructure

The surfaces of the polished fracture test bars were examined to determine the material integrity. This was accomplished with a B&L metallograph. Any inclusions, porosity, etc. observed were noted. Scratch/dig measurements were also made on optically polished surfaces by the approach described in Mil-0-13830 at 200 times magnification.

2.3.7 Optical Absorption Coefficient

A CO₂ laser calorimeter was used to obtain an accurate measure of the bulk optical absorption coefficient for germanium at 10.6 μm. This computer automated equipment which has been described by Bernal⁴ uses a CO₂ laser that can produce a maximum power output of 300 watts and can evaluate parts to 22 inches in diameter. Each germanium sample was inserted into the calorimeter, thermally stabilized about ten minutes and then the laser was turned on (power setting about 4 watts) for about 10 minutes. The temperature rise and fall of the sample was recorded as a function of time and the absorption coefficient (β) was computed from Equation (5).

$$\beta = \frac{K}{p} \cdot \frac{dx}{dt} \text{ where } K = \frac{cm(Efs)T}{d(Xfs)(SF)} \quad (5)$$

p = input power

m = mass

c = specific heat

d = thickness of sample

$\frac{dx}{dt}$ = heating cooling slope

Efs = full scale voltage

T = theoretical transmission

Xfs = full scale deflection

SF = scale factor conversion

2.3.8 Preshape Fabrication

The four preshaping approaches described below were evaluated by using one inch flat discs.

2.3.9 Conventional Preshaping

Six ground Bridgeman grown discs were obtained to simulate the standard preshaping method used in the optical industry. This approach simulated either an initial curve generated surface as performed by the germanium blank supplier or an in-house grinding operation.

2.3.10 Casting

Casting was proposed as an approach for obtaining preshaped blanks of germanium without the knowledge that this process had been used, to a limited extent, by Exotic Materials and possibly by Eagle-Picher. Exotic's cast material was obtained in simple flat disc shapes to evaluate this approach. Six samples were obtained where one surface was replicated against a flat graphite mold.

2.3.11 Hot Deformation

Six curve generated, convex/concave discs shaped as in Figure 2-1b were obtained from Exotic Materials. These were then hot deformed in the carbon tube, resistive heated furnace shown in Figure 2-2. Flat discs were used to simulate the opposite condition where curve generated preshaped lens blanks are supplied. This approach was based on an expired patent issued to Gallagher^{5,6} in 1959 and on preliminary internal development work at Honeywell performed with silicon in 1976. The curved blanks were deformed to flat blanks at $865 \pm 10^\circ\text{C}$ over a period of three to five hours at maximum stresses under 1500 psi.

2.3.12 Casting and Hot Deformation

Six curve generated blanks of Exotic's replicated cast germanium were purchased and also hot deformed as described above. Both approaches forged curved pieces to a flat condition to facilitate the final single point diamond turned optical finishing operation.

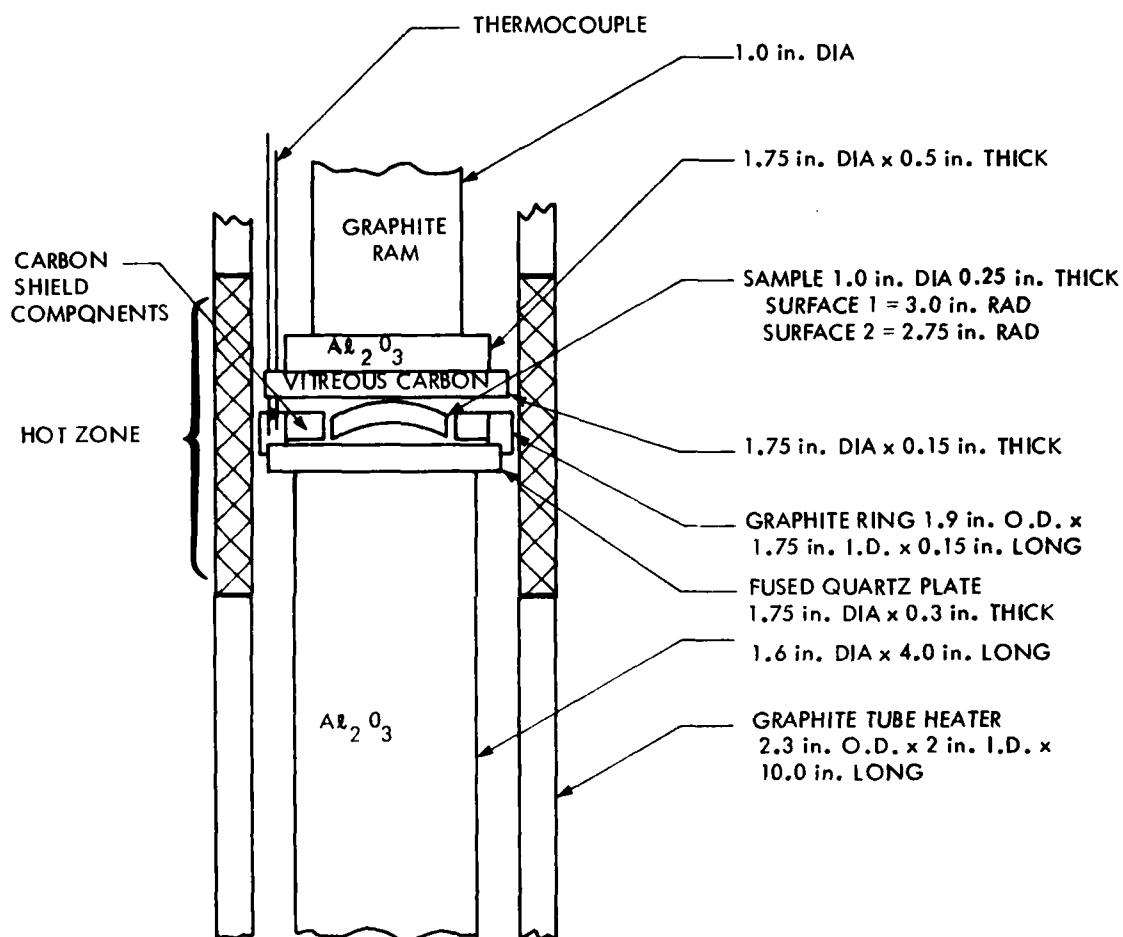


Figure 2-2. Hot Deforming Apparatus

2.3.13 Optical Finishing

Each of the flat discs, preshaped as described above, were then optically finished by either conventional polishing or single point diamond turning (SPDT), as described below.

2.3.14 Conventional Polishing

Three to four discs for each of the four preshaping approaches were sanded flat and parallel, first on wet 400 grit and then on 600 grit silicon carbide sand paper to a common thickness of 0.127 inch. The parts were then ultrasonically cleaned and mounted in clusters of seven on a 3-1/2" flat plate. Initial polishing was performed with 0.5 μ m alumina and kerosene on Pellon Pan-w lap. Final polishing was done with 0.5 μ m alumina and water on a paraffin lap.

2.3.15 Single Point Diamond Turning

Two discs from each of the four preshaping approaches were also sanded flat and parallel to a common thickness of 0.129 inch and then 0.002 inch from each surface was removed by single point diamond turning. At this point in the program, Honeywell only had the capability to turn optically flat surfaces such as that shown in Figure 2-3. This Pneumo Precision Incorporated flycutting lathe is a single axis machine where the single point diamond is mounted on the flywheel about five inches off center. This flywheel is mounted on an air bearing spindle which is rotated at about 2000 rpm. The samples were mounted on a right angle bracket atop an air bearing slide with double-sided sticky tape. The slide was translated past the flycutter at a linear rate of 1 ipm to produce the desired surface in germanium. While this was the only equipment available at the time of this effort, Honeywell now has a contouring capability to diamond turn aspheric germanium lenses to specification requirements.

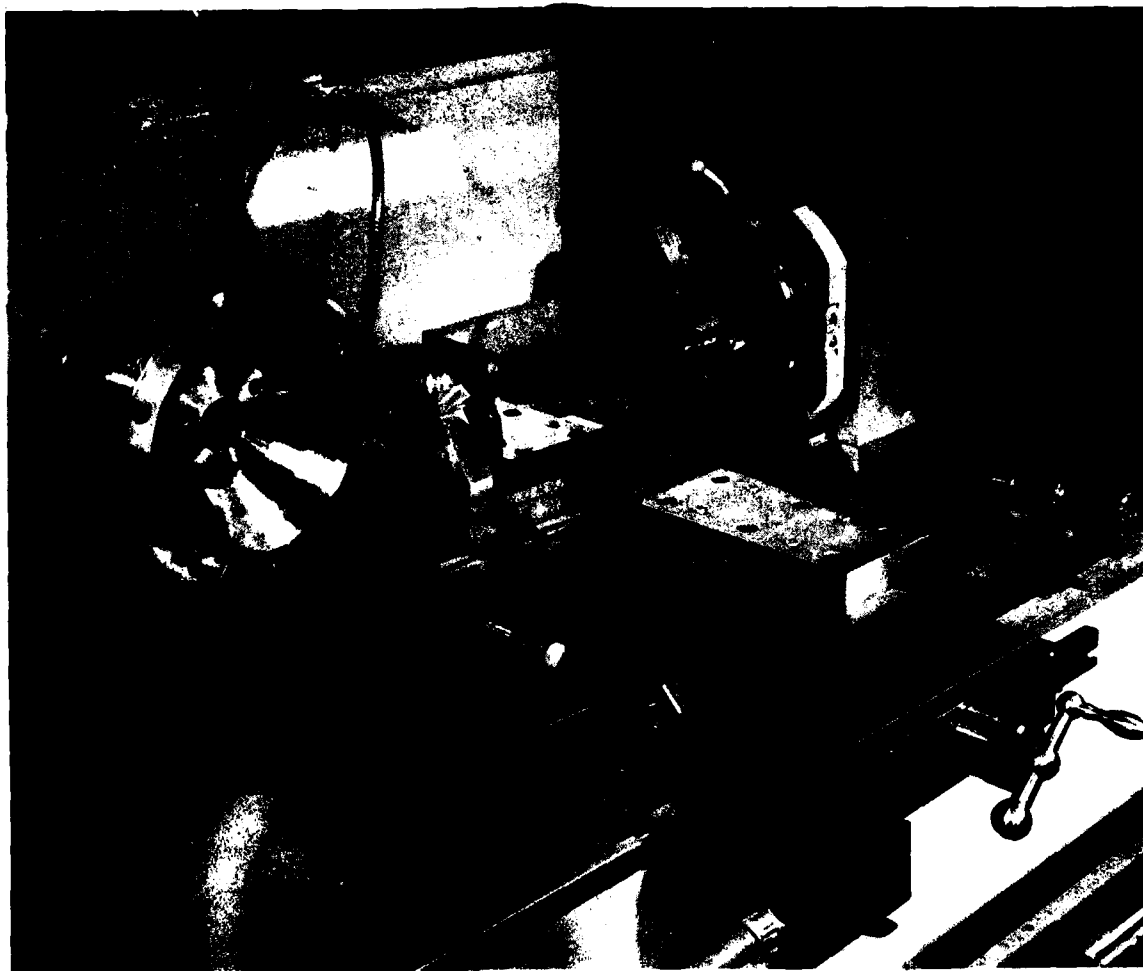


Figure 2-3. Single Point Diamond Turning (SPDT) of Four-Surface Mirror

2.3.16 Testing and Evaluation

All of the optically polished and single point diamond turned parts were then evaluated for infrared transmission, optical absorption coefficient, mechanical strength, electrical resistivity, scratch/dig and flatness before an antireflective (AR) coating was applied. The optical transfer function (OTF) was obtained after AR coating. Those new tests which were not described previously are outlined below.

2.3.17 Flatness

The flatness of each surface was measured with a Davison Model D-309 Interferometer using a 5461A filtered light source. This non-contact approach was capable of evaluating the single point diamond turned samples equally as well as the conventionally polished samples.

2.3.18 Optical Transfer Function (OTF)

Two diamond turned and three to four conventionally polished samples produced by each of the four approaches studied were evaluated for OTF after they had been AR coated by Spectra Scientific⁷. Figure 2-4 shows the OTF equipment that was first used to measure the baseline germanium aspheric lens. Measurements were taken at 10 micron increments along the focal plane until the best focus was found. Each flat sample evaluated was then placed in front of the lens at best-focus and the OTF was recorded. The OTF of the aspheric lens was then compared with each of the flat sample tests.

The selected target was mounted at the focus of the collimator and an Infrared Industries Blackbody with an 8 to 12 μm filter was used to illuminate the target. A chopper between the target and source modulated the signal at 13 Hz, the peak frequency response of the thermopile used as the detector in the OTF system. Although the samples were coated to reduce reflectance, they were also mounted at a slight angle to the optical axis to eliminate second surface reflectance. An aperture stop 0.7 inch in diameter was mounted on the lens bench in front of the aspheric lens and the OTF of the lens was measured at

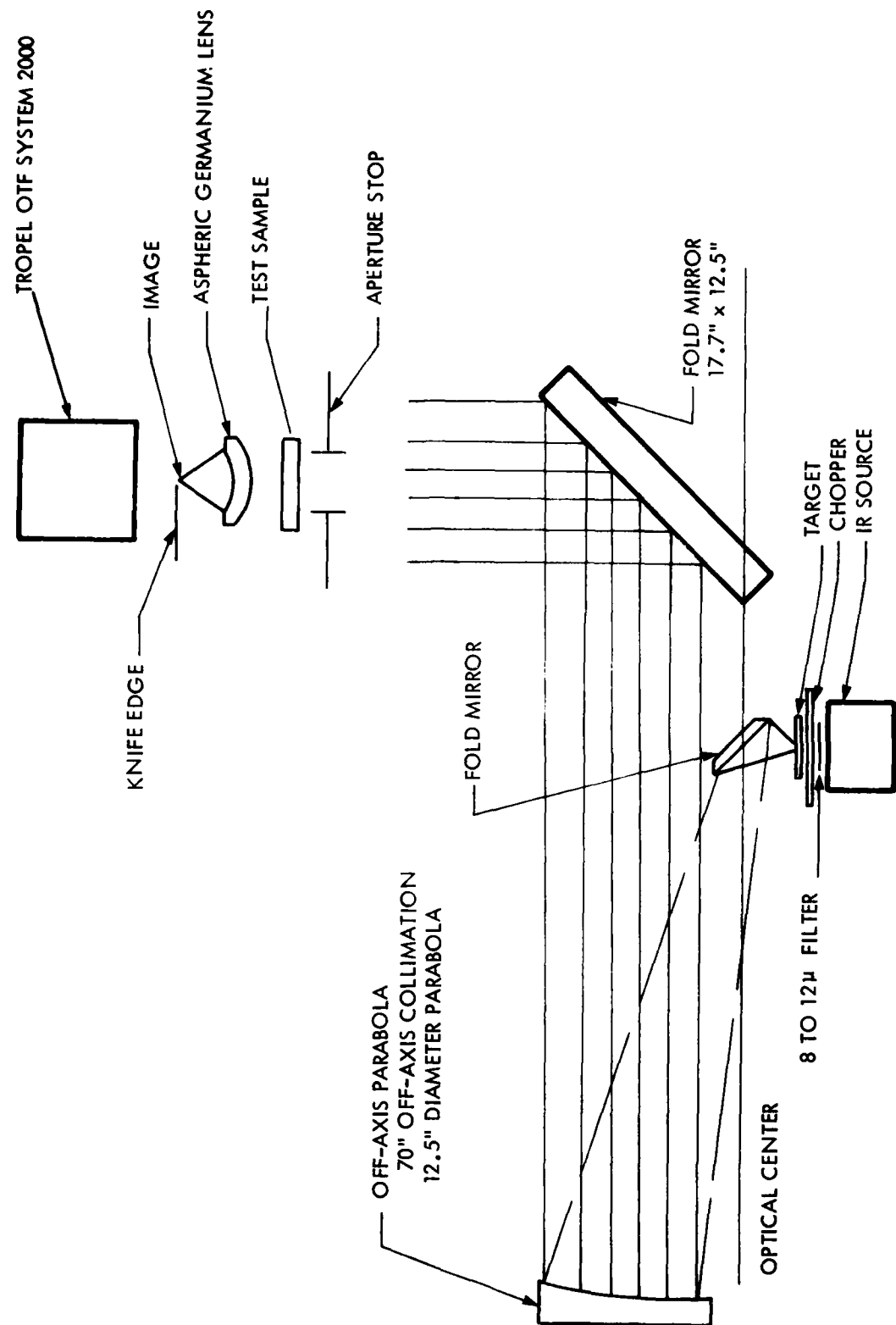


Figure 2-4. OTF Test Equipment Setup

best focus. The sample to be evaluated was then mounted on the lens bench between the 0.7 inch stop and the aspheric lens and the OTF was again measured. This measurement was repeated for each sample. After the last sample was measured, the OTF of the lens only was again measured to verify the test setup.

2.3.19 Cost Analysis

Four approaches were analyzed to determine which of these would potentially yield the most cost effective fabrication approach to be pursued in the second task of this program. The material costs were based on quotes obtained from Eagle Picher for quantities of 1000/month in 1978. It was assumed that acquisition cost was 4.5%, material evaluation cost was \$40.80/kgm, and that the salvage value of machine waste and scrapped lenses was \$230/kgm. It was also assumed that each lens would be made one at a time, all tooling and equipment was available and all labor and burden rates were constant for each process. The processing cost for the hot deformation and casting approaches were assumed to be the same, while the material costs were assumed to be higher for the hot deformation approach. The yields were based on the estimated degree of difficulty expected for the particular type of lens. It was also assumed that the conventional approach was the only approach which required a rough grinding operation.

SECTION 3

RESULTS AND DISCUSSION

3.1 CONVENTIONAL LENS GENERATING PROCESSES

The conventional processing steps that are used for fabricating spherical surfaces on germanium infrared lenses are given in Figure 3-1. In this process, cylindrical blanks of germanium are procured as specified in drawing SM-C-773478¹. As shown in Figure 3-2 a lens such as SK-AB114-2 uses only about 30 percent of the germanium in the blank. The other 70 percent can be reclaimed; however, only about 85 percent of the germanium's value is recovered.

The present method of generating a lens from the germanium blank is to use grinding tools to take off the major part of the material. A cup grinding tool is spun by one shaft while the germanium blank is spun by a second shaft. Depending on where the spin axes cross, the surface generated will be convex or concave, and the radius of curvature will be controlled by the inclination of the two axes as shown in Figure 3-3. The surfaces are brought to the desired radius by this rough grinding process. The surfaces are then ready for the fine grinding and polishing operations.

The effort examined in this interim period established the most cost effective, technically acceptable approach to use for generating the rough shaped lens blank. Two hot forming processes, casting and hot deformation, were studied. The combination of casting and hot deformation was also examined. First, the technical feasibility of these three approaches was compared with that of the conventional process and then the cost implication of each process was examined.

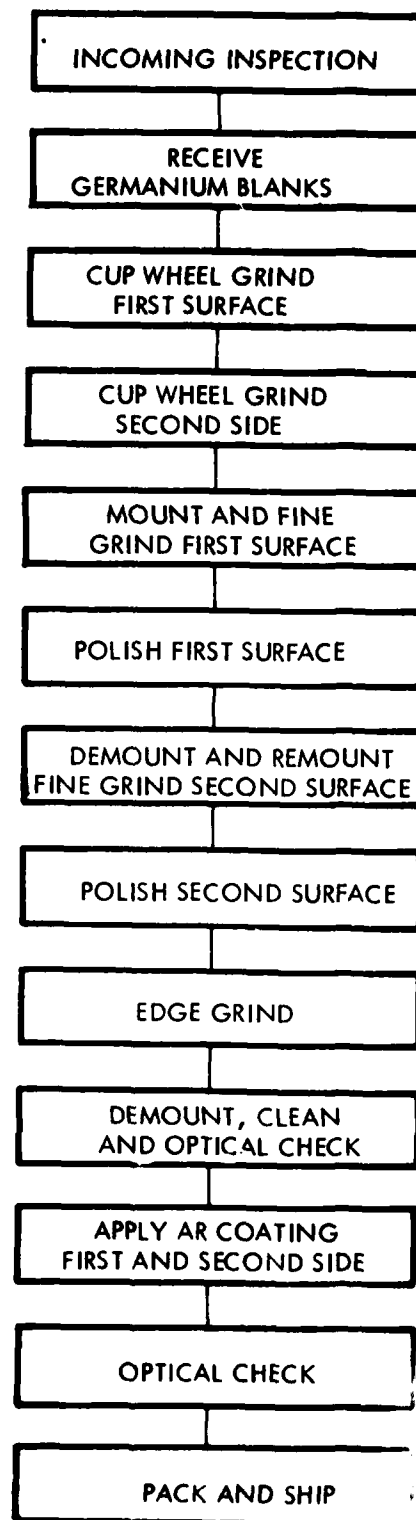


Figure 3-1. Present Germanium Lens Fabrication

Flow Diagram



Figure 3-2. Lens Forming From Germanium Blank

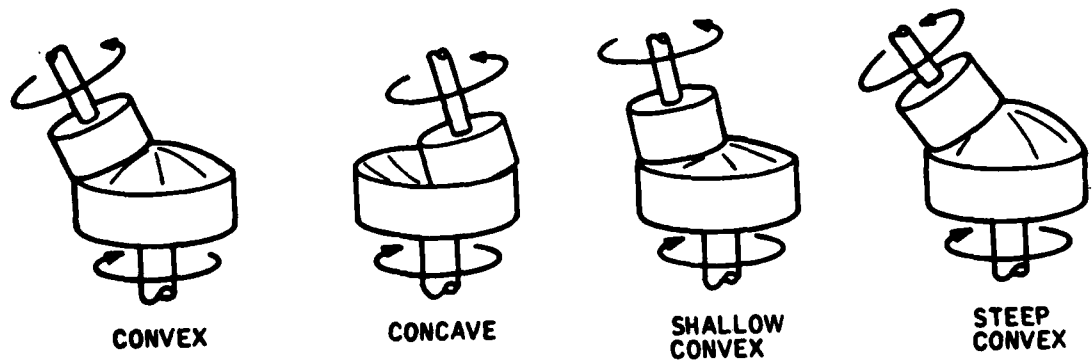


Figure 3-3. Conventional Methods of Generating Lenses

3.2 HOT DEFORMATION AND CASTING PROCESSES

The concept of casting optical materials to the desired lens radii has been shown to be possible for a wide variety of materials such as glass, alkaline earth fluorides⁷ and silicon⁸. It was not known until after the start of this program that casting of germanium had been used to form certain types of lenses. Exotic Materials³ advised that they had this capability; therefore, the cast materials studied in this effort were obtained from this source. Later Eagle-Picher² reported that they also use this process, but none of their cast material was evaluated.

3.2.1 Comparison Between Deformation of Alkali Halides and Germanium

This current program evaluated the feasibility of producing hot deformed cylindrical blanks of germanium.

Germanium is brittle at room temperature, but it has been known for some time that this covalently bonded material readily deforms at elevated temperatures^{6,9}. Since the major point of this discussion relates to the feasibility of forging germanium into shapes suitable for IR optical elements, a comparison of the deformation behavior of germanium and the alkali halides is in order. The alkali halides (e.g., KCl) are also brittle at room temperature but have been quite successfully forged into IR optical elements at elevated temperatures.⁴ Materials with the rock salt structure slip on $\{110\} \langle 110 \rangle$ systems at room temperature. Only two of the $\{110\} \langle 110 \rangle$ slip systems are independent, and five are needed to maintain strain continuity during forging.⁹ Thus alkali halides must be worked at high temperatures where slip also occurs on $\{100\} \langle 110 \rangle$ systems. The added slip systems provide the five necessary for strain continuity and forging to high strains without fracturing⁴.

In germanium, the situation is different. Germanium has the diamond cubic crystal structure and deforms by slip on $\{111\} \langle 110 \rangle$ systems¹⁰, i.e., the same slip systems that operate in face centered cubic metals. There are 12 independent $\{111\} \langle 111 \rangle$ systems, and strain continuity is not a problem. Germanium is brittle at room temperature because of the strong covalent bonding in

the structure. The lattice resistance to the propagation of dislocations is high and the yield stress at ordinary temperatures generally exceeds the fracture stress. At elevated temperatures, however, the resistance is overcome by thermal activation and the material can be plastically deformed.

Germanium can be deformed at temperatures exceeding about 500°C (Figure 3-4). Two predominate deformation mechanisms operate at high temperatures. At high strain rates and stresses, deformation occurs by the conservative motion of dislocations by glide through the lattice. In germanium, the stress above which deformation occurs only by glide is about $10^{-12}G$, where G is the shear modulus¹¹ or 75,400 psi. At stresses lower than this and at strain rates usually encountered in slow forging operation, germanium most likely deforms by dislocation creep¹¹. In dislocation creep, deformation results from dislocation glide and diffusion-controlled climb around obstacles^{11,12}. The deformed microstructure consists of dislocations aggregated into cells or subgrains.

3.2.2 Hot Deformation of Germanium Discs

The first hot deforming test made was on standard Eagle-Picher Bridgeman grown germanium. A 1.5 inch curve-generated disc (Figure 2-1a) was loaded with 175 psi. At 940°C some edge melting occurred, but about 25% of the deformation required to flatten the curved disc did take place. A second curve generated disc of this material loaded at 170 psi was heated to 850°C and 90% deformation took place.

No reaction on sticking of the germanium with the fused quartz on glassy carbon die materials was observed in these first tests. Edge melting in the first run also made contact with a graphite surface; however, no reaction or sticking between these materials was detected. All of the materials used in the hot deformation apparatus appeared to be satisfactory.

The twelve curve generated Exotic 1.0 inch discs (Figure 2-1b) were hot deformed flat under the conditions given in Table 3-1. Temperatures of 855 to 875°C were used where the final pressure applied was about 1000 psi. The average rate of center deflection took place at 1.4×10^{-4} in/min. There

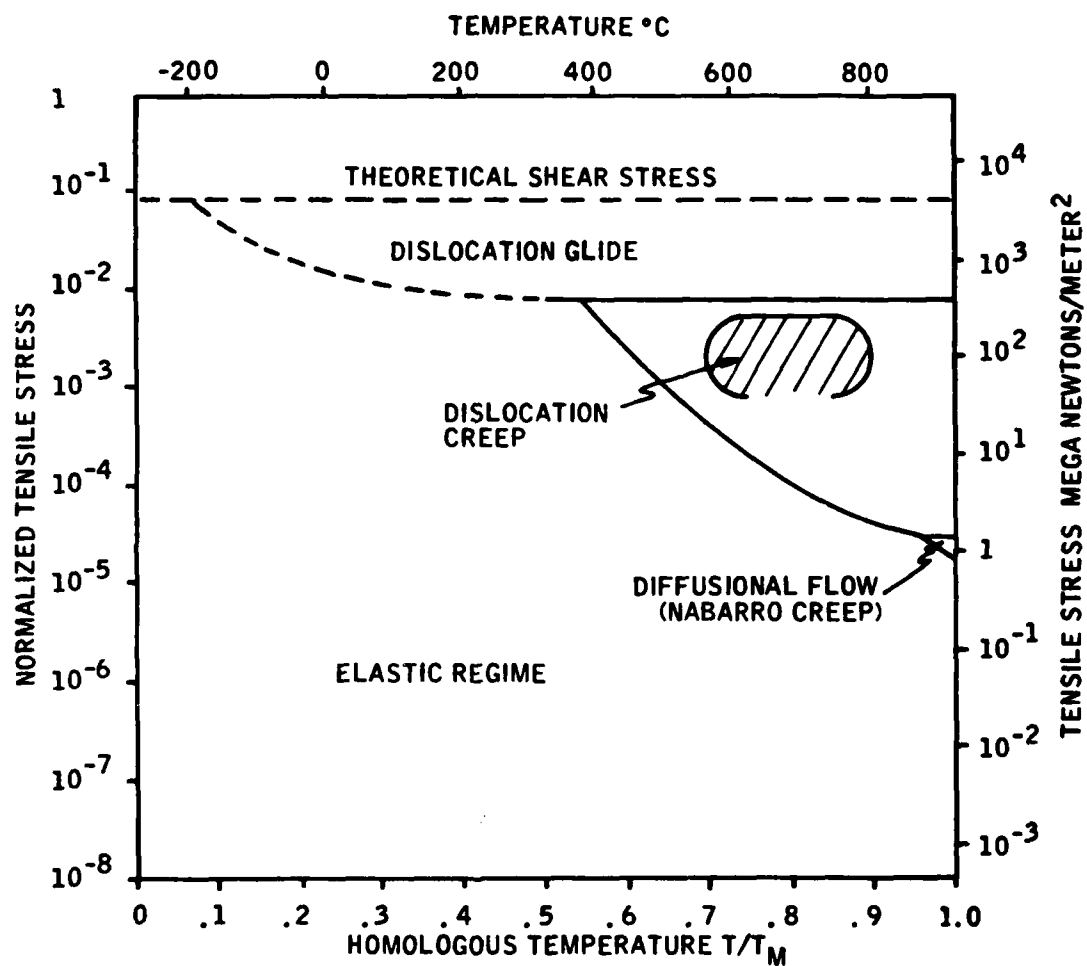


Figure 3-4. Deformation Mechanism Map for Germanium

Table 3-1. PROCESS DATA ON OPTICAL EVALUATION PARTS

PROCESS	SAMPLE NO.	HOT DEFORMATION		% COMPLETE		% TRANSMISSION		FINISHING PROCESS	ELECTRICAL RESISTIVITY ohm-cm	MODE OF RUPTURE p.s.i	OPTICAL ABSORPTION 10.6 μm /cm	MORSE SCRATCH/DIG NO.	FLATNESS IN VISIBLE
		TEMP °C	TIME (MIN)			8.0 μm	11.9 μm						
Cast Ge Exotic	01-1	-	-	-	-	-	-	SPDT	-	-	9.5	-	$\lambda/16-\lambda/8$
	01-2	-	-	-	-	-	-	SPDT	-	-	15.8	-	$\lambda/16$
	01-3	-	-	-	-	49.0	46.2	CONV	-	-	5.0	1/0	$\lambda/2-3\lambda/4$
	01-4	-	-	-	-	48.9	45.8	CONV	-	-	14.1	8/0	$3\lambda/2-\lambda/8$
	01-5	-	-	-	-	49.5	46.6	CONV	-	-	7.3	2/0	$\lambda/4-3\lambda/4$
	01-6	-	-	-	-	48.1	45.2	CONV	14.9	24,683	-	-	-
Bridgeman Ge Exotic	02-1	-	-	-	-	-	-	SPDT	-	-	13.3	-	$\lambda/8$
	02-2	-	-	-	-	-	-	SPDT	-	-	14.6	-	$\lambda/8-\lambda/4$
	02-3	-	-	-	-	49.2	46.3	CONV	-	-	4.8	1/0	$\lambda/8-\lambda/2$
	02-4	-	-	-	-	48.8	46.0	CONV	-	-	4.1	<1/0	$\lambda/4-\lambda/2$
	02-5	-	-	-	-	49.3	46.4	CONV	-	-	6.2	<1/0	$\lambda/4-\lambda/2$
	02-6	-	-	-	-	48.0	45.1	CONV	4.3	25,353	-	-	-
Hot Deformed Cast Ge Exotic	03-1	855/865	160/245	38/84	-	43.9	40.6	CONV	20.7	29,895	-	-	$\lambda/4-\lambda/2$
	03-2	855	187	95	-	46.5	43.4	CONV	-	-	23.8	1/0	$\lambda/4-\lambda/2$
	03-3	875	235	90	-	43.5	39.9	CONV	-	-	37.9	2/3	$\lambda/4-\lambda/2$
	03-4	865	226	88	-	-	-	SPDT	-	-	28.4	-	$\lambda/16$
	03-5	860	267	90	-	-	-	SPDT	-	-	14.9	-	$\lambda/16$
	03-6	870	329	93	-	46.6	43.5	CONV	-	-	20.4	2/1	$\lambda/8-\lambda/2$
Hot Deformed Bridgeman Ge Exotic	04-1	860	220	70	-	47.0	44.0	CONV	16.8	30,600	-	-	-
	04-3	855	228	83	-	-	-	SPDT	-	-	26.9	-	$\lambda/16$
	04-4	865	317	88	-	-	-	SPDT	-	-	42.4	-	$\lambda/16$
	04-5	855	212	90	-	44.0	40.4	CONV	-	-	44.8	4/0	$\lambda/2$
	04-6	870	268	81	-	46.2	43.0	CONV	-	-	32.1	2/0	$\lambda/4-\lambda/2$
	EP-1 EP-2	- -	- -	- -	-	48.3	45.2	CONV	16.2	23,798	-	-	-
Bridgeman Ge Eagle-Picher						-	-	-	-	-	5.0	-	-

appeared to be little difference between the deformation behavior of these two materials. Only one of the twelve parts was damaged (04-2). This was caused by a malfunction in the furnace controls. Thus, the technique of hot deformation (as conceived by Gallagher⁶) with cast on Bridgeman grown germanium was confirmed.

3.2.3 Casting and Hot Deforming of Germanium Lens Blanks

Additional work was also done to demonstrate the feasibility of casting and hot deforming germanium lens blanks: 1) Twenty grams of germanium powder (99.999% Eagle Pitcher 1st reduction 100 mesh) was melted in an Argon atmosphere into a high purity graphite mold (Figure 3-5) at 955°C for 30 min and then directionally solidified (cooled at 2°/min from bottom to top) by the natural thermal gradient in the furnace. The part formed is shown in Figure 3-6. 2) Two flat discs (1.5 inches diameter by 0.125 inch thick) of Eagle Picher Bridgeman grown material with several grain boundaries, were hot deformed in the apparatus shown in Figure 3-5 into the concave/convex lens blanks shown in Figure 3-6. The radii of these surfaces, 1.01 and 1.22 inches respectively, were accomplished at $875 \pm 5^\circ\text{C}$ with a load of 800 pounds. While both of these approaches have been shown to be feasible as a shaping operation, additional effort was required to determine if these processes were detrimental to the optical behavior of the material.

3.2.4 Polishing and Single Point Diamond Turning of Germanium

The ability to conventionally polish and single point diamond turn these materials was evaluated with the flat discs produced above. Table 3-1 lists the electrical, physical, and optical properties determined for the material obtained or produced for this phase of the program. All parts were optically finished to a thickness of 0.125 inch by conventional polishing and single point diamond turning (SPDT).

The precision of the SPDT process is very apparent. Note the surface flatness achieved with SPDT was usually better than $\lambda/8$ in visible light as opposed to about $\lambda/2$ for the conventionally polished samples. Flatter, more consistent surfaces, obviously, could have been obtained with the standard polishing process; however, this was not required for this study.

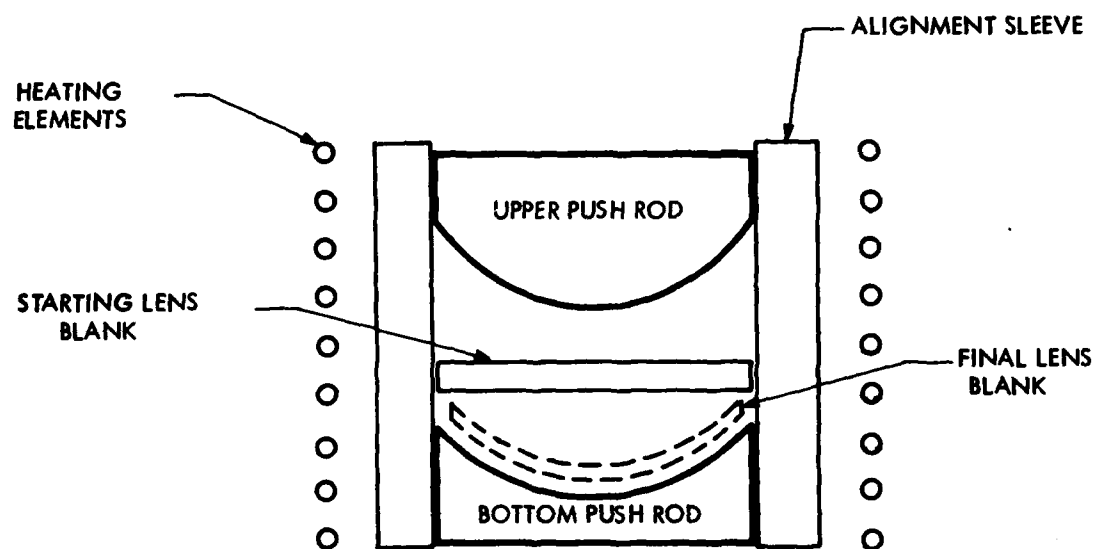
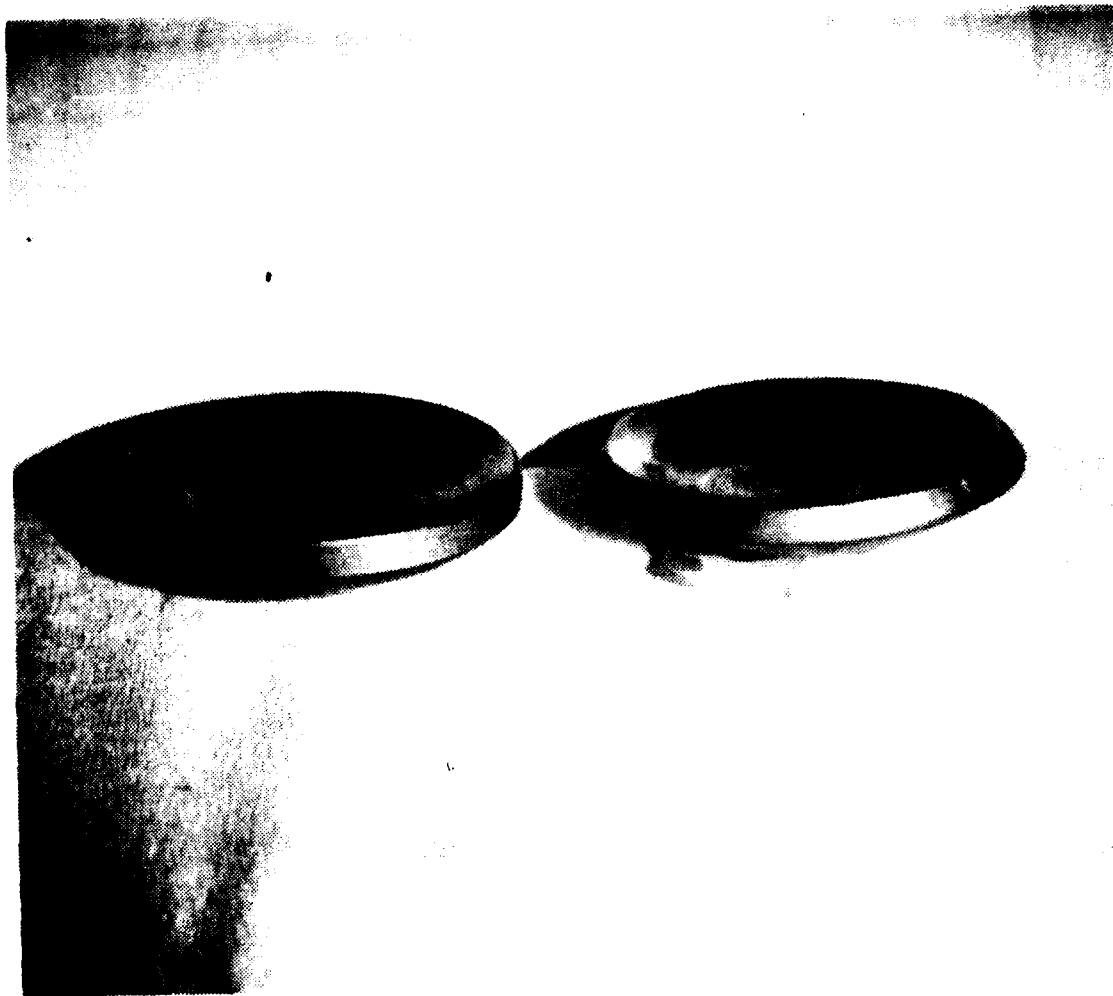


Figure 3-5. Hot Deformation of Lens



(a) Casting

(b) Hot Deformed

Figure 3-6. Germanium Lens Blanks (a) Casting, (b) Hot Deformed

3.2.5 Evaluation of Optically Polished Germanium

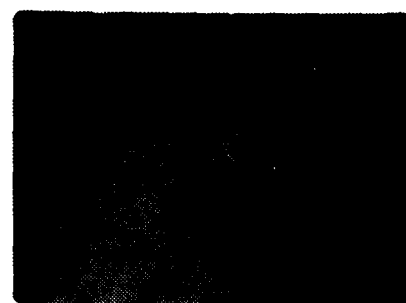
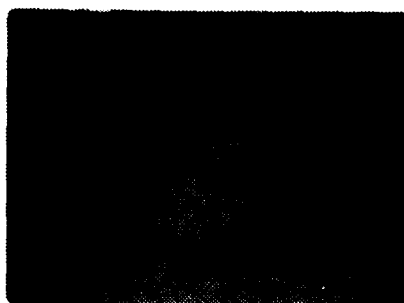
The standard scratch/dig method for evaluating optically polished surfaces was based on the width in micrometers over the number of digs greater than 10 μm . The values reported in Table 3-1 represent worst case observed at 200 times magnification. Typical areas for a sample produced by each process are shown in Figure 3-7a. Most of the conventionally polished surfaces had scratches less than one micrometer in width with the worst case observed being 8 micrometers. Digs greater than 10 micrometers were generally not present but one sample did contain three digs.

The SPDT process produced a high-quality, mirror-like optical finish when observed without the aid of a microscope. However, at the 200 times magnification shown in Figure 3-7b the surface can be seen to contain many small pull-out pits that are generally less than one micrometer which would not be classified as digs (must be greater than 10 micrometers). These pits were observed to be larger and more heavily concentrated for grains with one type of crystal orientation in the cast or hot deformed germanium.

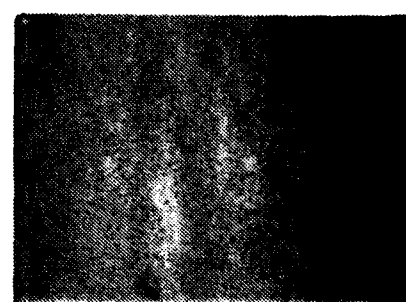
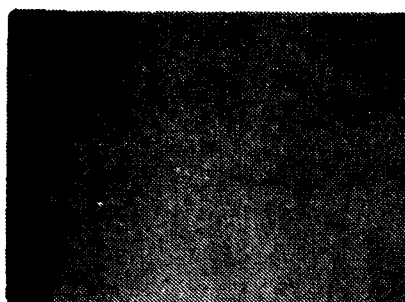
The applicability of diamond turning to the generation of infrared optical quality surfaces in germanium has been demonstrated by Johnson and Saito¹³. Honeywell conducted a program for the Air Force Materials Laboratory (AFML) where Rank Optics Ltd. fabricated a diamond-turned germanium aspheric detector lens using their standard two-step technique: a) figuring on their R- θ turning machining and then, b) performing a post-turning, automatic compliant lap for final polish. Performance testing of this element satisfied system design goals for spot-size and OTF.

The infrared transmission over the range of 5 to 16.7 micrometers of typical samples of each material is shown in Figure 3-8. There was no apparent difference between the Eagle Picher Bridgeman grown and Exotic cast germanium materials. However, there was substantial optical absorption in the hot deformed material at wavelengths greater than 6.3 micrometers. The percent transmission (with reflection losses) at 8 and 11.9 micrometers was therefore used to compare each sample in Table 3-1. The average optical transmission

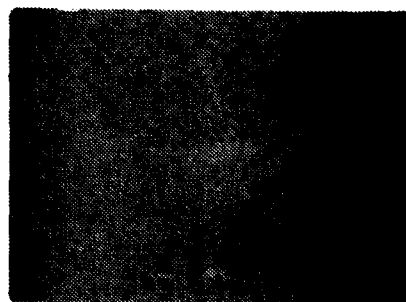
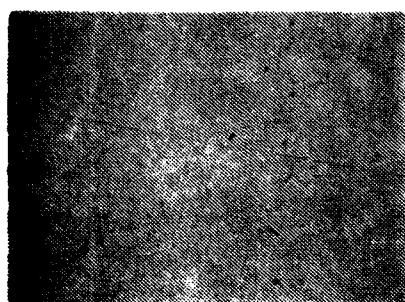
01-CAST Ge



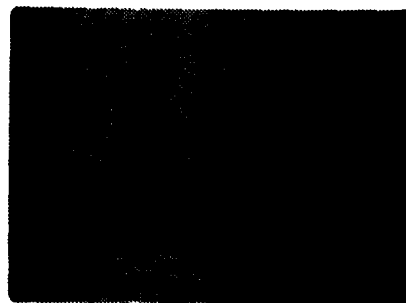
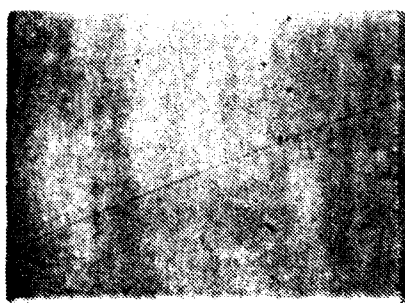
02-BRIDGEMAN
GROWN Ge



03 HOT
DEFORMED
CAST Ge



04-HOT
DEFORMED
BRIDGEMAN
GROWN Ge



(A) CONVENTIONALLY POLISHED

(B) SINGLE POINT DIAMOND TURNED

Figure 3-7. Photomicrographs of Finished Germanium (x 200 magnification)

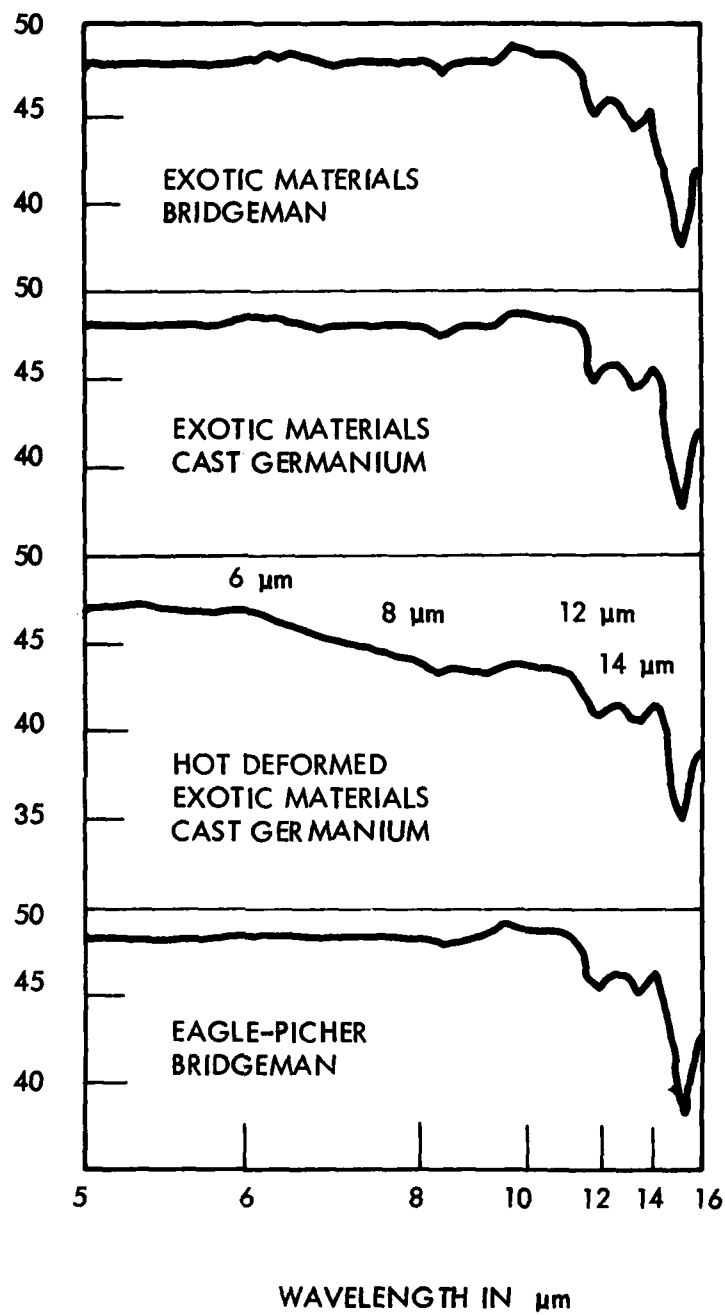


Figure 3-8. Plots of Infrared Optical Transmission of Germanium

over these wavelengths was essentially the same for both sources of Bridgeman grown germanium and the Exotic cast material. However, the transmission through both hot deformed materials was about 7 percent less than normally processed germanium.

The calorimetrically determined optical absorption data obtained at 10.6 micrometers showed a similar trend. About 10 percent absorption per centimeter of thickness occurred in the standard materials; whereas the hot deformed cast and Bridgeman grown materials had 25 to 36 percent absorption, respectively, at 10.6 micrometers.

The exact reason for the higher absorption and low transmission in the hot deformed germanium is not understood at this time. A more thorough study as to the cause and prevention of this phenomenon is beyond the scope of this program.

The average mechanical strength (Table 3-1) in bending of these materials was shown to be about 24,000 to 25,000 pounds per square inch (psi) for the standard materials. However, the two materials produced by the hot deforming process had strengths which averaged about 30,000 psi. It is interesting to note that the strength increased as the optical absorption at 10.6 micrometers increased. If dislocations or vacancies were introduced in the material during hot deformation, an increase in strength would certainly be expected and increased optical absorption may also occur.

The electrical resistivity of each material was distinctly different. Exotic materials Bridgeman grown germanium was lower (4.3 ohm-cm) than their cast germanium (14.9 ohm-cm), but both of these were lower than the Eagle-Picher Bridgeman grown germanium (16.2 ohm-cm). The values obtained for the hot deformed material were 20.7 and 16.8 ohm-cm for the cast and Bridgeman grown materials, respectively. The detrimental nature of this process also affected electrical resistivity.

It has been concluded that more effort on hot deformation of optical grade germanium needs to be done before this process can be considered for manufacturing preshaped lenses.

An initial attempt was made to measure the OTF of uncoated optically finished flat discs; however, high reflection losses made this impossible. All samples were, therefore, AR coated and then measured in a system where an aspheric lens was used as a reference point. The characteristics of the aspheric lens before and after testing the flat discs were measured. As the spatial frequency increased, more variability between the two runs occurred. At 15 lines/mm (the specified spatial frequency for the FLIR system being studied in this program) there was a difference of about 6 percent between the two runs. Thus, this OTF approach was accurate to about $\pm 3\%$.

Table 3-2 gives a summary of the OTF data obtained. Inserting flat discs in the test system caused a 8 to 10 percent drop in modulus with conventional optical finishing as opposed to 5 to 8 percent loss with the SPDT approach. At longer spatial frequencies, the Bridgeman grown material appeared to yield parts which were slightly better than those produced by casting. Hot deforming these materials did not appear to have a significant influence on OTF. However, the SPDT surface finishing appeared to produce slightly better OTF. Apparently, the OTF is most strongly influenced by the flatness and parallelism of the surfaces generated. Therefore, OTF does not appear to have been impacted significantly by the types of fabrication processes being studied in this program.

3.3 COST ANALYSIS

The factory cost for material, labor and burden was determined for four manufacturing processes: casting, hot deformation, purchased preshaped blanks and conventional grinding. Table 3-3 gives the cost estimate for each of the seven lenses considered for this program based on a production rate of 1000 per month using 1978 cost for labor and material.

It can be seen that the casting approach usually was the most economical process; however, the hot deformation approach was about the same for concave/convex shaped lenses. Neither process had a significant advantage for shallow or small lens shapes such as AB108-1 and AB108-2.

Table 3-2. OTF DATA

MATERIAL	AVERAGE % MODULUS AT SPATIAL FREQUENCY (LINES/MM)									
	1.9	3.7	5.6	7.5	9.4	11.2	13.1	15.0	16.9	18.7
Exotic Cast Ge	93	83	79	74	71	69	66	60	57	53
Hot Deformed Cast Ge	91	82	79	77	74	70	64	59	57	52
Exotic Bridgeman Ge	92	84	81	82	79	73	67	65	60	59
Hot Deformed Bridgeman Ge	93	86	83	79	74	70	65	60	58	54
Aspheric Baseline Lens	99	95	90	86	82	76	71	69	64	56
SPDT Finish	93	85	81	78	75	71	67	62	60	56
Conventional Finish	91	82	80	77	72	69	64	59	55	52

Table 3-3. MMAT COST ANALYSIS SUMMARY*

Dollars Each in Lots of 1000

Type Lens	108-1	108-2	114-1	114-2	115-1	115-2	116-2
Lens Size Dia. X Thick	3.26x0.30	1.0x0.11	2.60x0.20	1.80/0.192	2.00/0.075	2.00/0.165	2.50/0.25
<u>MFG. PROCESS</u>							
Process A Casting	323	171	268	137	226	206	254
Process B Hot Deforming	337	168	268	140	235	208	261
Process C Preshape Blanks	330	171	304	160	272	236	272
Process D Conventional	365	231	368	197	370	287	303

Basic Assumptions:

1. Factory Cost without G&A and Fee
2. Each Lens Made One at a time
3. No grinding operations required except in Process D
4. Tooling & Equipment are available to meet production rates
5. Material Acquisition Rate is 4.5%
6. All labor and burden rates are constant for each process
7. Material Evaluation Cost \$40.80/KgM
8. Material Salvage is \$230/KgM
9. Rate in 1000 lenses per month

NOTES:

☐ Recommended
☒ Approach

* SEE APPENDIX FOR DETAILED
 COST ANALYSIS FIGURES

Using preshaped blanks was less expensive than the conventional rough grinding approach. All three of these approaches became more cost effective than the conventional rough grinding approach. The smaller the radius of a lens, the greater the cost savings. For instance, the savings with AB115-1 with an approximate radius of 1.7 inch was \$144 or 40 percent as opposed to only \$49 or 16 percent for AB116-2 with radii greater than 3.5 inches.

No attempt was made to show the cost advantage of single point diamond turning (SPDT) over conventional polishing for the aspheric surface finishing. No practical volume production polishing approaches were known for aspheric finishing. A comparison between AB114-2 and 115-2 shows the cost of the SPDT process for an aspheric surface to be about \$70 more than a conventional polished spherical surface.

More details on the cost breakdown for these lenses has been generated in a separate report to the Night Vision and Electro-Optics Laboratory at Fort Belvoir.

SECTION 4

CONCLUSIONS

It has been shown that casting and hot deforming of germanium can be used to form lens blanks that are close to the initial shapes required for fine grinding and then polishing. Hot deforming of germanium at 870°C causes a three-fold increase in optical absorption at 10.6 μm , but only about 7 percent loss in infrared transmission over the 8 to 11.9 μm wavelength. This degradation appears to be caused by dislocations or vacancies which are introduced by this process. There was also an increase of electrical resistivity and a slight decrease in optical transfer function, but there was an improvement in mechanical strength.

Casting appeared to be the most cost effective approach for lenses with a strong radius of curvature for four of the seven lenses considered in this program. Whereas small or shallow lenses, in which very little material is lost during grinding, can be best obtained in the preshaped configuration produced by the primary germanium source company.

Single point diamond turning appeared to be the most attractive finishing approach for aspheric surfaces; whereas conventional polishing was more cost effective for spheric surfaces.

SECTION 5

RECOMMENDATIONS

Four of the seven lenses considered for this program can be most readily fabricated by the casting method; however, extensive tooling would have to be designed and built to supply the limited number of lenses required for the remainder of this program. It is therefore recommended that all of the germanium blanks should be bought in the pre-shaped condition. The remaining effort should place emphasis on the tooling and processes required to generate aspheric surfaces by single point diamond turning on a numerically controlled two axes machine.

APPENDIX A REFERENCES

1. W.B. Harrison, "Manufacturing Methods and Technology for Optical Fabrication," Honeywell First Quarterly Report DAAB07-77-C-0615, July 1978.
2. Eagle-Picher Industries, Inc., Compounds and Metals Department, P.O. Box 737, Quapaw, Oklahoma 74362.
3. Exotic Materials, Inc., 2968 Randolph Ave., Costa Mesa, California 92626.
4. E. Bernal G., et al., "Preparation and Characterization of Polycrystalline Halides for Use in High Power Laser Windows," Honeywell Final Report on DARPA Contract Nos. DAHC-15-72-C-0227 and DAHC-15-73-C-0464, 20 February 1978.
5. C.J. Gallagher, "Methods of Plastic Working of Semiconductors," U.S. Patent No. 2,725,318, 29 November 1959.
6. C.J. Gallagher, Phys. Rev. 88, (1952), p. 721.
7. R. Newberg and J. Pappis, "Fabrication of Fluoride Laser Windows by Fusion Casting," Proc. Fifth Conf. on Infrared Laser Window Materials (December 1975), p. 1066.
8. P. Stello and R. Griest, "Optical Properties of Cast Polycrystalline Silicon," Proc. IRIS, 4 (1959), p. 101.
9. J.R. Patel and B.H. Alexander, Acta. Met. 4 (1956), p. 385.
10. G.W. Groves and A. Kelly, Phil. Mag. 8 (1963), p. 877.
11. M.F. Ashby, Acta. Met. 20 (1972), p. 887.
12. A.G. Evans and T.G. Langon, Prog. Mat. Sci. 21 (1976), p. 171.
13. F.E. Johnson and T.T. Saito, "Applications of Diamond Turning to Infrared Optical Systems," SPIE 93 (1976).

APPENDIX B GLOSSARY OF TERMS

Afocal - An optical system whose object and image point are at infinity.

Anti-reflective(AR)Coatings - A single or multilayer coating applied to a surface or surfaces of a substrate to decrease the reflectance of the surface and increase the transmission of the substrate over a specified wavelength range.

Casting - A method by which a molten material is formed, solidified, and then cooled in a confining die or mold.

Diffusional Flow - The spontaneous movement of atoms to an extent sufficient to cause mass flow of material.

Dislocation Glide - The slip or movement of atoms along planes through dislocations in bulk material.

Dislocations - Defects in the atomic lattice of a crystal represented by the presence of excess atoms or absence of atoms in the normal perfect atomic structure of material.

Dispersion - The process by which rays of light of different wavelengths are deviated angularly by different amounts as with prisms and diffraction gratings. Also applied to the other phenomena that cause the index of refraction and other optical properties of a medium to vary with wavelength.

Form-to-Shape - A forming process that converts an irregular shape of a material into a predetermined final shape as defined by a die or mold cavity.

Homologous Temperature - The relationship (ratio) between the working temperature of a material and its melting point, both in degrees absolute.

Hot Deforming - The deforming of a material above its recrystallization temperature which is sufficient to cause bending and distortion of that material into a permanent new shape.

Imager - A single or multiple set of optical elements that form an image by collecting a bundle of light rays diverging from an object point and transforming it into a bundle of rays converging toward another point.

Infrared - The electromagnetic radiation beyond the red end of the visible spectrum (0.768 to 40 μm). Heat is radiated in the infrared region. The FLIR ranges of interest are 3 to 5 μm and 8 to 14 μm .

Interference - A term used to denote the additive process, whereby the amplitudes of two or more overlapping waves are systematically attenuated and reinforced.

Interferometer - An instrument employing the interference of light waves for purposes of measurement, such as the accuracy of optical surfaces by means of Newton's rings, the measurement of optical paths, and linear and angular displacements.

Modulation - A measure of the variation of illuminance across an image of a sine wave object. Defined as $M = (I_{\max} - I_{\min}) / (I_{\max} + I_{\min})$ where I_{\max} and I_{\min} are the maximum and minimum illuminance in the image.

Modulation Transfer Function (MTF) - The function describing the modulation intensity of the image of a sinusoidal object with increasing frequency. It describes the results obtained on passing through an optical system. Also called "sine wave response" and "contrast transfer function."

Optical Transfer Function (OTF) - The function describing modulation and spatial phase shift of the image of a sinusoidal object with frequency as the independent variable as a result of passing through an optical train.

Sag - Abbreviation for sagitta, the height of a curve measured from the chord (as applied to optics).

Single Point Diamond Turning (SPDT) - A relatively new turning technique that uses precision spindles and movements (usually air bearing movements), and a high speed single point diamond turning tool that can be moved in microinch stages. This technique has been shown to be especially useful for turning metal mirrors as well as other optical components.

Special Phase Shift - The displacement of the image of a sine wave object from its ideal position. Usually measured in degrees, with 360 degrees assigned to a full cycle of the image.

Thermal Imaging - A representation of an object's thermal profile by means of its infrared (IR) rays.

APPENDIX C
DETAILED COST FIGURES FOR MANUFACTURING METHODS
AND TECHNOLOGY FOR OPTICAL FABRICATION

FACTORY COST BREAKDOWN FOR PROCESS A - CASTING

Type Lens	Dollars per 1000						
	108-1	108-2	114-1	114-2	115-1	115-2	116-2
Lens Size Dia. X Thick	3.26 x 0.30	1.0 x 0.11	2.6 x 0.20	1.80 x 0.192	2.00 x 0.075	2.00 x 0.165	2.50 x 0.25
Lens Weight in Kgm/1000	194	7.78	87.6	36.7	38.8	41.8	123
Germanium							
Material Cost -- Germanium	132,211	11,020	69,943	30,571	39,659	34,662	71,846
Material Cost -- Process	13,879	2,248	9,179	4,815	5,829	5,829	8,809
Process Cost	176,791	157,677	188,518	101,788	180,960	165,263	173,303
Total Cost	322,881	170,945	267,640	137,174	266,448	205,754	253,958
Including							
Aspheric Cost	37,683	66,663	56,492	0	62,769	47,072	47,072
AR Coating Cost	78,375	14,001	66,593	36,146	49,408	49,408	60,426
Other Processing Cost	74,612	79,281	74,612	70,457	74,612	74,612	74,612

FACTORY COST BREAKDOWN FOR PROCESS B -- HOT DEFORMING

Type Lens	Dollars per 1000						
	108-1	108-2	114-1	114-2	115-1	115-2	116-2
Lens Size Dia. X Thick	3.26 x 0.30	1.0 x 0.11	2.6 x 0.20	1.80 x 0.192	2.00 x 0.075	2.00 x 0.165	2.50 x 0.25
Lens Weight in Kgm/1000	194	7.78	87.6	36.7	38.8	41.8	123
Germanium							
Material Cost -- Germanium	145,927	8,398	70,224	32,943	48,295	36,679	79,126
Material Cost -- Process	13,879	2,248	9,179	4,815	5,829	5,829	8,809
Process Cost	176,791	157,677	188,518	101,788	180,960	165,263	173,303
Total Cost	336,597	168,323	267,921	139,546	235,084	207,771	261,238
Including							
Aspheric Cost	37,683	66,663	56,492	0	62,769	47,072	47,072
AR Coating Cost	78,375	14,001	66,593	36,146	49,408	49,408	60,426
Other Processing Cost	74,612	79,281	74,612	70,457	74,612	74,612	74,612

FACTORY COST BREAKDOWN FOR PROCESS C -- PRESAPED

Type Lens	Dollars per 1000						
	108-1	108-2	114-1	114-2	115-1	115-2	116-2
Lens Size Dia. x Thick	3.26 x 0.30	1.0 x 0.11	2.6 x 0.20	1.80 x 0.192	2.00 x 0.075	2.00 x 0.165	2.50 x 0.25
Lens Weight in Kgm/1000	194	7.78	87.6	36.7	38.8	41.8	123
Germanium							
Material Cost -- Germanium	145,945	17,049	113,371	60,149	91,592	71,247	96,489
Material Cost -- Process	13,461	1,804	8,761	4,426	5,411	5,411	8,391
Process Cost	170,536	151,813	182,263	95,186	174,705	159,008	167,048
Total Cost	329,942	170,666	304,395	159,761	271,708	235,666	271,928
Including							
Aspheric Cost	37,683	66,663	56,492	0	62,769	47,072	47,072
AR Coating Cost	78,375	14,001	66,593	36,146	49,408	49,408	60,426
Other Processing Cost	69,939	72,953	67,939	63,466	67,939	67,939	67,939

FACTORY COST BREAKDOWN FOR PROCESS D -- CONVENTIONAL

Type Lens	Dollars per 1000						
	108-1	108-2	114-1	114-2	115-1	115-2	116-2
Lens Size Dia. X Thick	3.26 x 0.30	1.0 x 0.11	2.6 x 0.20	1.80 x 0.192	2.00 x 0.075	2.00 x 0.165	2.50 x 0.25
Lens Weight in Kgm/1000	194	7.78	87.6	36.7	38.8	41.8	123
Germanium							
Material Cost -- Germanium	143,803	12,107	129,246	59,535	129,329	75,040	80,223
Material Cost -- Process	13,555	2,001	8,896	4,529	5,590	5,545	8,525
Process Cost	208,274	216,597	230,253	132,942	234,856	206,684	214,723
Total Cost	365,632	230,705	368,393	197,006	369,775	287,269	303,471
Including							
Aspheric Cost	37,683	74,453	58,590	0	69,461	48,855	48,855
AR Coating Cost	78,375	13,425	66,593	36,146	49,408	49,408	60,427
Other Processing Cost	105,771	130,712	113,966	101,325	121,577	113,966	113,966

APPENDIX D DISTRIBUTION LIST

DELS-D-PC Commander Defense Documentation Center ATTN: DDC-TCA Cameron Station, Building 5 Alexandria, VA 22314	12
Commander US Army Material Development and Readiness Command ATTN: DRCRD-MT 5001 Eisenhower Avenue Alexandria, VA 22333	2
Office of Defense Research & Engineering Communications and Electronics Room 3D1037 Washington, DC 20330	1
Director US Army Production Equipment Agency ATTN: Mr. C. McBurney Rock Island Arsenal Rock Island, IL 61299	1
Department of Defense Deputy for Science & Technology Ofc of Assist Sec Army (R&D) Washington, DC 20310	1
Advisory Group on Electron Devices 201 Varick Street, 9th Floor New York, NY 10014	2
Chief, Research & Development ATTN: Director of Developments Department of the Army Washington, DC 20310	1

Dr. James a. Tegnalia 1
Defense Advanced Research
Projects Agency
1400 Wilson Blvd.
Arlington, VA 22209

Commander 1
US Army Research Office
ATTN: DRXRO-IP
P.O. Box 12211
Research Triangle Park
North Carolina 27709

Central Intelligence Agency 1
ATTN: DRS/Add/Publications
Washington, DC 20505

Commander 1
US Army Missile Command
Redstone Scientific Info. Center
ATTN: Chief, Document Section
Redstone Arsenal, AL 35809

US Army Missile Commander 1
ATTN: DRSMI-RGP (Mr. Victor Ruwe)
Redstone Arsenal, AL 35809

Commander 1
Harry Diamond Laboratories
ATTN: Mr. Horst Gerlach
ATTN: U(DRXDO-RAA)
2800 Powder Mill Road
Adelphia, MD 20783

Director 1
Defense Intelligence Agency
ATTN: DI-5C3
Washington, DC 20301

Director 1
Defense Mapping Agency
ATTN: DMA/PRA
Washington, DC 20305

Commander 1
Naval Electronics Laboratory Center
ATTN: Library
San Diego, CA 92152

Commander
Department of the Navy, ELEX 05143A
ATTN: A.H. Young
Electronics System Command
Washington, DC 20360

1

Chief
Naval Ship Systems Command
Department of the Navy
ATTN: Code 681A2b, Mr. L. Gumina
Room 3329
Washington, DC

1

Commander
US Naval Air Development Center
ATTN: Library
Johnsville, Warminster, PA 18974

1

HQDA
ATTN: DAMA-CSC-ST (Maj R. Andrews)
Room 3D43
Pentagon
Washington, DC 20310

1

Commander
Air Research & Development Command
ATTN: RDTCT
Andrews Air Force Base
Washington, DC

1

HQDA (DAMA-WSA)
ATTN: LTC Waddel
Washington, DC 20310

1

Commander
US Army Training & Doctrine Command
ATTN: ATCD-S1
Fort Monroe, VA 23651

2

Commander
US Army Training & Doctrine Command
ATTN: ATCD-C1-1
Fort Monroe, VA 23651

1

CDR, US Army Development &
Readiness Commander
ATTN: DRCMA-EE
5001 Eisenhower Avenue
Alexandria, VA 22333

1

D-3

8008-5

Commander US Army Missile Command ATTN: DRSMI-RR (Dr. J.P. Hallows) Redstone Arsenal, AL 35809	1
NASA Scientific & Tech Information Facility P.O. Box 8757 Baltimore/Washington Int'l Airport	2
National Aeronautics & Space Administration George C. Marshall Space Flight Center ATTN: R-QUAL-FP ATTN: U (Mr. Leon C. Hamiter) Huntsville, AL 35812	1
NASA - Manned Space Craft Center Reliability and Flight Safety Division ATTN: Library Houston, TX	1
Commander US Armament Command ATTN: DRSAR-RDP (Library) Rock Island, IL 61201	1
Commander US Army Combined Arms Combat Developments Activity ATTN: ATCAIC-IE Fort Leavenworth, KS 66027	1 1
Bell Laboratories Whippany Road ATTN: Tech Reports Center, WH5E-227 Whippany, NJ 07981	1
Commander US Army Intelligence School ATTN: ATSIT-CTD Fort Sill, OK 73503	1
Commandant US Army Engineer School ATTN: ATSE-CTD-DT-TL Fort Belvoir, VA 22060	1

Commander Picatinny Arsenal ATTN: SARPA-TS-S No. 59 Dover, NJ 07801	1
US Army Research Office-Durham ATTN: CRDARD-IP Box CM, Duke Station Durham, NC 27706	1
US Army Research Office-Durham ATTN: Dr. Robert J. Lontz Box CM, Duke Station Durham, NC 27706	1
Directorate of Combat Developments US Army Armor School ATTN: ATSB-CD-AA Fort Knox, KY 40121	1
Honeywell Incorporated ATTN: Dr. Rudolph C. Oswald 13350 US 19 St. Petersburg, FL 33733	1
USA Security Agent ATTN: LARD Arlington Hall Station Arlington, VA 22212	1
Commander US Army Tank-Automotive Command ATTN: DRSTA-RW-L Warren, MI 48090	1
Commandant US Army Air Defense School ATTN: C & S Dept, Msl Sci Div Fort Bliss, TX	1
Commander US Army Combined Arms Combat Developments Activity ATTN: ATCACC Fort Leavenworth, KS 66027	1
Dr. Robert H. Rediker Massachusetts Institute of Technology Building 13-3050 Cambridge, MA 02139	1

Northrop Corporation Laboratories ATTN: Library 320-61 3401 West Broadway Hawthorne, CA 90250	1
Rockwell International Corporation Science Center Thousand Oaks, CA	1
Hughes Aircraft Corporation ATTN: Mr. D. Hartman Building 100 MSA 788 P.O. Box 90515 Los Angeles, CA 90009	1
Commander US Army Missile Command ATTN: DRSMI-RE (Mr. Pittman) Redstone Arsenal, AL 35809	1
Commander US Army Systems Analysis Agency ATTN: DRXS-T, Mr. A. Reid Aberdeen Proving Ground, MD 21005	1
Commander US Army Tank-Automation Command ATTN: DRSTA-RHP, Dr. J. Parks Warren, MI 48090	1
Commander US Army Materials and Mechanics Research Center ATTN: DRXMR-M (N.H. Fahey) Watertown, MA 02172	1
Commandant US Army Aviation School ATTN: ATZQ-D-MA (O. Heath) Fort Rucker, AL 36360	1
Office of Naval Research ATTN: DR. D.K. Perry Arlington, VA 22217	1
Commander US NAval Air Systems Command ATTN: AIR 335 (Mr. E. Cosgrove) Washington, DC 20361	1

Commander
US Navy Weapons Center
Michelson Lab
ATTN: Code 6018 (H.E. Barnett)
China Lake, CA 93555

1

Director
Naval Research Laboratory
ATTN: Code 2627
Washington, DC 20375

1

Commandant
Marine Corps
HQ, US Marine Corps
Washington, DC 20380
ATTN: Code LMC

1

HQ, US Marine Corps
ATTN: Code INTS
Washington, DC 20380

1

Raytheon
Research Division
28 Seyon Street
Waltham, MA 02154

1

Eagle Picher
Miami Research Labs
ATTN: Mr. Paul E. Grayson
200 Ninth Avenue, NE
Miami, OK 74354

1

Department of the Air Force
Office of Scientific Research
1400 Wilson Blvd.
Arlington, VA 22209

1

Ballistic Missile Radiation
Analysis Center
Env Research Inst of Michigan
Ann Arbor, MI 48107

1

Hughes Aircraft Company
ATTN: Mr. A. Berg
MS-C106
Building 6
Culver City, CA 90230

1

Battelle Pacific Northwest Labs Optics, Lasers and Holography ATTN: Dr. B.P. Hildebranch Richland, WA 99352	1
Grumman Aerospace Corp. Research Dept. and Advanced Development Department Bethpage, NY 11714	1
Director Optical Sciences Center University of Arizona Tucson, AZ 85721	1
Director US Army Night Vision & Electro-Optics Laboratories ATTN: DELNV-SI (Mr. D. Helm) Fort Belvoir, VA 22060	3
Bell & Howell ATTN: Mr. George R. McGee 7100 McCormick Road Chicago, IL 60645	1
Pacific Optical 3221 West 102nd Street Los Angeles, CA	1
Special Optics Little Falls, NJ	1
Ovel Corporation 15 Market Street Stamford, CT	1
Esco Optics Products 111 Oak Ridge Road Oak Ridge, NJ	1
Millis Girot 3006 Entripuse Street Costa Mesa, CA	1
Commander US Army Combined Arms Combat Developments Activity ATTN: ATCAIC-IE Fort Leavenworth, KS 66027	1